

# Perturbative and non-perturbative aspects of the non-abelian Boltzmann-Langevin equation

Dietrich Bödeker <sup>1</sup>

*Fakultät für Physik, Universität Bielefeld, D-33615 Bielefeld*

## Abstract

We study the Boltzmann-Langevin equation which describes the dynamics of hot Yang-Mills fields with typical momenta of order of the magnetic screening scale  $g^2T$ . It is transformed into a path integral and Feynman rules are obtained. We find that the leading log Langevin equation can be systematically improved in a well behaved expansion in  $\log(1/g)^{-1}$ . The result by Arnold and Yaffe that the leading log Langevin equation is still valid at next-to-leading-log order is confirmed. We also confirm their result for the next-to-leading-log damping coefficient, or color conductivity, which is shown to be gauge fixing independent for a certain class of gauges. The frequency scale  $g^2T$  does not contribute to this result, but it *does* contribute, by power counting, to the transverse gauge field propagator. Going beyond a perturbative expansion we find 1-loop ultraviolet divergences which cannot be removed by renormalizing the parameters in the Boltzmann-Langevin equation.

PACS numbers: 11.10.Wx, 11.15.-q

---

<sup>1</sup>e-mail: bodeker@physik.uni-bielefeld.de

# 1 Introduction

We consider hot non-abelian gauge fields at a temperature  $T$  sufficiently large so that the the running coupling  $g = g(T)$  is small. Even then gauge fields with typical momenta of order  $g^2 T$ , the so called magnetic screening scale, are strongly coupled [1]. Despite this, physical quantities have an expansion in powers of  $g$  times possible logarithms of  $g$ . Only the coefficients in this expansion cannot be calculated perturbatively when they receive contributions from magnetic scale momenta. For example, the order  $g^6$  contribution to the free energy comes with a non-perturbative coefficient. This coefficient can be calculated by a lattice simulation of 3-dimensional pure Yang-Mills theory, which was shown by using dimensional reduction [2]. This technique can only be applied to static quantities, like the free energy or equal time correlation functions.

In this paper we consider dynamical quantities, which are determined by unequal (real) time correlation functions. While the free energy is sensitive to the magnetic scale only at relatively high order in the weak coupling expansion, there are dynamical quantities which are determined by this scale at leading order. An important example is the Chern-Simons diffusion rate in unbroken non-abelian gauge theories, often referred to as the hot sphaleron rate. In the standard electroweak theory it determines the rate for anomalous baryon number violation above the electroweak phase transition or cross-over temperature  $T_c \sim 100$  GeV <sup>2</sup>. It is a crucial ingredient in scenarios which try to explain the baryon asymmetry of the universe, e.g., through leptogenesis [3] or electroweak baryogenesis [4]. In QCD Chern-Simons diffusion leads to non-conservation of quark helicity even in the chiral limit [5]. Another physical quantity which is sensitive to the magnetic screening scale at leading order is the friction experienced by an electroweak phase transition bubble wall [6].

Euclidean lattice simulations are of limited use for calculating real time observables <sup>3</sup>, and real time simulations of quantum field theory are not possible. However, even for dynamical quantities one can use perturbation theory to integrate out short distance modes to obtain an effective theory for the non-perturbative long-distance dynamics. The first step is to integrate out “hard” physics associated with virtual momenta of order  $T$ . At leading order in the gradient expansion one obtains the so called hard

---

<sup>2</sup>Close to  $T_c \sim 100$  one must take the Higgs field into account [7] unless the transition is strongly first order.

<sup>3</sup>Recently methods have been developed for obtaining real time correlation functions from Euclidean lattice simulations using the so called maximal entropy method [8]. However, this cannot be applied to Chern-Simons diffusion which is exponentially suppressed in Euclidean time.

thermal loop effective theory [9]. The remaining degrees of freedom are gauge fields with characteristic wave vectors  $\mathbf{k} \lesssim gT$ . Their occupation number  $n(|\mathbf{k}|) = 1/(e^{|\mathbf{k}|/T} - 1) \simeq T/|\mathbf{k}|$  is large which means that they can be treated as classical fields. This opens the possibility for a non-perturbative treatment because classical field theories can be treated on the lattice in real time [10]. The hard thermal loop effective theory was used for non-perturbative lattice simulations [11]-[13] which, however, do not have a continuum limit [14].

One can, however, go further using perturbation theory. Integrating out all frequency scales and spatial momenta <sup>4</sup> larger than  $g^2T$  one finds that at leading order in  $g$  the dynamics of gauge fields  $A^\mu$  is described by the Boltzmann-Langevin equation [15]

$$(C + v \cdot D)\widetilde{W} + \frac{d}{m_D^2}(c_1 + \mathbf{v} \cdot \mathbf{D})\mathbf{v} \cdot \mathbf{D} \times \mathbf{B} = \mathbf{v} \cdot \mathbf{E} + \xi, \quad (1.1)$$

which is a classical field equation for  $A$  and  $\widetilde{W}$ .  $D_{ab}^\mu = \delta_{ab}\partial^\mu - g f_{abc}A_c^\mu$  is the covariant derivative in the adjoint representation,  $E^i = F^{i0}$  and  $B^i = -\frac{1}{2}\epsilon^{ijk}F^{jk}$  are the non-abelian electric and magnetic fields.  $m_D$  is the Debye or electric screening mass which is of order  $gT$ , and  $d$  denotes the number of spatial dimensions. We choose  $d = 3 - \epsilon$  to regularize ultraviolet and infrared divergences.  $\widetilde{W}(x, \mathbf{v})$  transforms under the adjoint representation and represents color charge fluctuations of plasma particles with momenta of order  $T$  and velocity  $\mathbf{v}$ . We neglect fermion masses. Then these particles move at the speed of light so that  $\mathbf{v}^2 = 1$ . The 4-vector  $v$  is defined as  $v^\mu = (1, \mathbf{v})$ .  $C$  is a linear collision operator of order  $g^2T$  and depends logarithmically on the cutoff separating the scales  $gT$  and  $g^2T$ . It is local in space and acts only on the velocity variable,

$$Cf(\mathbf{v}) \equiv \int_{\mathbf{v}'} C(\mathbf{v}, \mathbf{v}')f(\mathbf{v}'). \quad (1.2)$$

Here  $\int_{\mathbf{v}}(\dots) \equiv \Omega^{-1} \int d^{d-1}v(\dots)$  is the normalized integral over the  $d - 1$  dimensional unit sphere,  $\Omega = 4\pi$  for  $d = 3$ .  $C$  commutes with rotations of  $\mathbf{v}$ . Therefore it can be diagonalized by expanding  $W(x, \mathbf{v})$  in spherical harmonics <sup>5</sup>  $Y_{lm}(\mathbf{v})$ , and the eigenvalues depend only on  $l$ . The  $l = 0$  eigenvalue vanishes, and the coefficient  $c_1$  in Eq. (1.1) is the  $l = 1$  eigenvalue.  $\widetilde{W}$  contains only spherical harmonics with respect  $\mathbf{v}$  with  $l \geq 2$ ,

---

<sup>4</sup>Since Lorentz invariance is lost at finite temperature, frequencies and spatial momenta have to be treated separately.

<sup>5</sup>Or their generalization in  $d \neq 3$  dimensions. To keep the terminology simple, we refer to them as spherical harmonics.

i.e.,

$$\int_{\mathbf{v}} v^\mu \widetilde{W}(x, \mathbf{v}) = 0. \quad (1.3)$$

$\xi(x, \mathbf{v})$  is a Gaussian white noise with the 2-point function

$$\langle \xi_a(x, \mathbf{v}) \xi_b(x', \mathbf{v}') \rangle = \frac{2T}{m_D^2} C(\mathbf{v}, \mathbf{v}') \delta_{ab} \delta^{d+1}(x - x'). \quad (1.4)$$

A non-trivial check of Eq. (1.1) is to see whether it reproduces the known thermodynamics of the magnetic scale gauge fields. In Ref. [15] it was indeed shown that Eq. (1.1) generates a thermal ensemble with a Boltzmann weight  $e^{-H/T}$  where

$$H = \frac{1}{2} \int d^3x \left\{ \mathbf{B}^2 + m_D^2 \int_{\mathbf{v}} \widetilde{W}^2 \right\}. \quad (1.5)$$

Thus for equal time correlation functions  $\widetilde{W}$  acts like a free field and does not affect the gauge fields. The term  $\frac{1}{2}\mathbf{B}^2$  is just the Lagrangian of the dimensionally reduced theory for the scale  $g^2T$  [2].

In the leading log approximation, neglecting terms suppressed by powers of  $[\log(1/g)]^{-1}$ , Eq. (1.1) can be replaced by a much simpler equation of motion which contains only the gauge fields [16],

$$\mathbf{D} \times \mathbf{B} = \gamma \mathbf{E} + \zeta. \quad (1.6)$$

Here  $\zeta$  is again a Gaussian white noise which is proportional to the  $l = 1$  projection of  $\xi$ . The damping coefficient  $\gamma$ , the color conductivity, is proportional to  $T/\log(1/g)$ . The only spatial momentum scale in Eq. (1.6) is  $\mathbf{k} \sim g^2T$ . Estimating the LHS as  $\mathbf{k}^2 \mathbf{A}$  and the first term on the RHS as  $\gamma k^0 \mathbf{A}$  one can see that the only frequency scale in Eq. (1.6) is  $k^0 \sim g^4T$  (modulo logarithms of the coupling). The Boltzmann-Langevin equation (1.1), on the other hand, contains two frequency scales,  $g^4T$  and  $g^2T$ , again modulo logarithms [15]. The question whether the frequency scale  $g^2T$  affects the non-perturbative gauge field dynamics has not been addressed so far.

Eq. (1.6) solves the notorious ultraviolet problems mentioned above. It is ultraviolet finite and has been used to calculate the hot sphaleron rate by Moore [17]. Its obvious disadvantage is that it's only valid in the logarithmic approximation. The Boltzmann equation which was obtained by integrating out the momentum scale  $gT$  [16]<sup>6</sup> and which served as a starting point for obtaining Eqs. (1.6) and (1.1) is valid to

---

<sup>6</sup> For a Feynman-diagram interpretation, see [18, 19].

leading order in  $g$  and all orders in  $[\log(1/g)]^{-1}$ , but it has the same 1-loop ultraviolet divergences as classical Yang-Mills theory. One can hope that Eq. (1.1) has a better ultraviolet behavior because it does not contain propagating gauge field modes which are responsible for these divergences.

An equation similar to (1.1) has been obtained by Arnold [20]. The difference between Arnold's Langevin equation and Eq. (1.1) is that the former does not contain a time derivative of  $\widetilde{W}$ . Thus in [20]  $\widetilde{W}$  is not dynamical, but it is fixed by  $A$  and  $\xi$  at the same instant of time. The only dynamical degrees of freedom are the gauge fields. On first sight this difference appears to be minor. However, if one discretizes time for solving these equations on the lattice with temporal lattice spacing  $\Delta x^0$  the two equations require rather different treatments. For Eq. (1.1)  $A$  and  $\widetilde{W}$  at time  $x^0 + \Delta x^0$  and spatial coordinate  $\mathbf{x}$  are determined by  $A$ ,  $\widetilde{W}$ , a finite number of their derivatives and  $\xi$ , all taken at  $x^\mu = (x^0, \mathbf{x})$ . This procedure is exactly the same as the one one would use for solving Eq. (1.6) [17]. For Arnold's Langevin equation, on the other hand, one first has to solve for  $\widetilde{W}$  at time  $x^0$ , so that  $\widetilde{W}(x^0)$  becomes a spatially non-local functional of  $A$  and  $\xi$  at time  $x^0$ . Then one can determine  $A(x^0 + \Delta x^0)$  from the so obtained  $\widetilde{W}(x^0)$  and from  $A(x^0)$  and  $\xi(x^0)$ . Since  $\widetilde{W}$  is linear in  $\xi$ , Arnold's Langevin equation can be viewed as a spatially non-local generalization of Eq. (1.6) in which the color conductivity  $\gamma$  and the noise  $\xi$  are gauge field dependent. The time discretization of such a Langevin equation is ambiguous, but it was argued in Ref. [20] that the ambiguity can be fixed by demanding that the equation yields the correct thermodynamics of magnetic scale gauge fields. In the path integral formulation of this equation (cf. Sec. 2) it is necessary to introduce additional terms in the action<sup>7</sup>. No such complications arise for Eq. (1.1).

Arnold and Yaffe used the Langevin equation of [20] to show that Eq. (1.6) is still valid at next-to-leading logarithmic order (NLLO), if one uses the next-to-leading logarithmic order (NLLO) color conductivity  $\gamma$ , which was calculated in Ref. [21]. It was argued that the additional terms in the path integral action mentioned above do not contribute at next-to-leading logarithmic order.

The purpose of this paper is three-fold. First, we want to study the large momentum behavior of Eq. (1.1) to see whether it is renormalizable. This is necessary if one wants to use Eq. (1.1) for non-perturbative lattice simulations and take the continuum limit. Secondly, we would like to understand whether Eq. (1.1) gives the same gauge field dynamics as the Langevin equation obtained by Arnold [20]. Finally we calculate the

---

<sup>7</sup>These terms are rather complicated. To quote the author of Ref. [20], 'they are ugly as sin'.

color conductivity at next-to-leading logarithmic order. We confirm the result obtained by Arnold and Yaffe [21], and we investigate its gauge fixing dependence.

To address these issues it is convenient to write the equation of motion (1.1) as a path integral. This method is briefly reviewed in Sec. 2 for a non-gauge theory. To apply it to Eq. (1.1) one has to fix the gauge which is discussed in Sec. 3. The path integral representation and the corresponding Feynman rules for Eq. (1.1) are obtained in Sec. 4. In Sec. 5 we study the large momentum behavior of the various propagators. We shall find 1-loop ultraviolet divergences which cannot be removed by renormalizing the parameters of the action (Sec. 5.1). In Sec. 6 we discuss the logarithmic approximation beyond leading order. Following Arnold and Yaffe we consider Wilson loops in Sec. 7 at next-to-leading logarithmic order (NLLO) to compute the NLLO color conductivity. In Sec. 8 we study the effect of the modes with  $k^0 \sim \mathbf{k} \sim g^2 T$  on the spatial gauge field propagator. Sec. 9 contains a summary and a discussion. In Appendix A we list some properties of the operator  $\hat{G}$  defined in Eq. (4.15). Appendix B describes the power counting for propagators and vertices used in Sects. 7 and 8. It also contains the approximated expressions for the propagators which are used in Sec. 7. The frequency integrals needed for the 1-loop selfenergies are listed in Appendix C. Appendix D contains the results for the individual 1-loop diagrams contributing to the  $A^0$  propagator which gives the dominant contribution to the Wilson loops discussed in Sec. 7.

**Notation** 4-vectors and 3-vectors are denoted by italics and boldface, respectively. The signature of the metric is  $(+ - - -)$ .

## 2 Path integral representation of Langevin equations

To investigate the properties of a Langevin equation it is convenient to re-write it as a path integral [22], which allows the use of the standard methods of quantum field theory. In this section we illustrate this method for a non-gauge theory. The fields are denoted by  $\varphi^i$  and  $i$  represents all indices including space and time variables. Similarly, we collectively label the components of the equation of motion with the index  $\alpha$ ,

$$\mathcal{E}^\alpha[\varphi] = \xi^\alpha. \quad (2.1)$$

We write the 2-point function of the noise as

$$\langle \xi^\alpha \xi^\beta \rangle = 2\tau \delta^{\alpha\beta}. \quad (2.2)$$

Physical observables are obtained by averaging over the noise with a Gaussian weight

$$\langle O \rangle = \int [d\xi] \exp \left\{ -\frac{1}{4\tau} \xi^\alpha \xi^\alpha \right\} O(\varphi_{\text{solution}}), \quad (2.3)$$

where  $\varphi_{\text{solution}}$  is the solution to the equation of motion (2.1). Now one introduces an integral over  $\varphi$  via

$$1 = \int [d\varphi] \det \left( \frac{\delta \mathcal{E}^\alpha}{\delta \varphi^i} \right) \delta(\mathcal{E} - \xi). \quad (2.4)$$

The  $\delta$ -function in (2.4) is represented by an integral over a Lagrange multiplier field  $\lambda$ ,

$$\langle O \rangle = \int [d\varphi \, d\xi \, d\lambda] \det \left( \frac{\delta \mathcal{E}^\alpha}{\delta \varphi^i} \right) \exp \left\{ -\frac{1}{4\tau} \xi^\alpha \xi^\alpha + i\lambda^\alpha (\mathcal{E}^\alpha - \xi^\alpha) \right\} O[\varphi]. \quad (2.5)$$

Finally one integrates over the noise and introduces ghost and anti-ghost fields  $\eta$  and  $\bar{\eta}$  to represent the determinant which gives

$$\langle O \rangle = \int [d\varphi \, d\lambda \, d\eta \, d\bar{\eta}] e^{-S} O[\varphi]. \quad (2.6)$$

The action

$$S = \tau \lambda^\alpha \lambda^\alpha - i\lambda^\alpha \mathcal{E}^\alpha - \bar{\eta}^\alpha \frac{\delta \mathcal{E}^\alpha}{\delta \varphi^i} \eta^i \quad (2.7)$$

is invariant under the BRST-transformation

$$\delta \varphi^i = \bar{\varepsilon} \eta^i, \quad \delta \bar{\eta}^\alpha = -i\bar{\varepsilon} \lambda^\alpha, \quad \delta \lambda^\alpha = \delta \eta^i = 0 \quad (2.8)$$

with the anti-commuting parameter  $\bar{\varepsilon}$ . This procedure can be applied to gauge theories, but first one has to fix the gauge.

### 3 Gauge fixing

Gauge covariant Langevin equations determine the gauge fields only up to a gauge transformation. Thus in order to use Eq. (2.4) to introduce a path integral one first has to fix a gauge. Zinn-Justin and Zwanziger [23] showed that the gauge condition

$$A^0(t) = v[\mathbf{A}(t)] \quad (3.1)$$

does not affect expectation values of gauge invariant operators  $O[\mathbf{A}]$ . A small variation

$$v[\mathbf{A}] \rightarrow v[\mathbf{A}] + \epsilon[\mathbf{A}] \quad (3.2)$$

can be compensated by a gauge transformation of  $A$ . It is easy to see that this result also holds for gauge invariant operators which depend both on the spatial gauge fields  $\mathbf{A}$  and on  $A^0$ .

A special case of (3.1) is

$$\kappa A^0 + \nabla \cdot \mathbf{A} = 0, \quad (3.3)$$

which smoothly interpolates between Coulomb ( $\kappa = 0$ ) and temporal gauge ( $\kappa \rightarrow \infty$ ). The free fields in this gauge are related to  $A^0$  in Coulomb gauge by

$$\begin{aligned} A^0(k) &= \frac{\mathbf{k}^2}{\kappa} \frac{i}{k^0 + i\mathbf{k}^2/\kappa} A_{\text{Coul}}^0(k), \\ \hat{\mathbf{k}} \cdot \mathbf{A}(k) &= \frac{|\mathbf{k}|}{k^0 + i\mathbf{k}^2/\kappa} A_{\text{Coul}}^0(k) \quad (\text{free fields}). \end{aligned} \quad (3.4)$$

With this relation we can obtain the propagators for the gauge (3.3) from the Coulomb gauge propagators listed in Sec. 4.1.

To obtain a path integral representation one can simply use the gauge condition (3.3) to eliminate  $A^0$  from the equations of motion, Eq. (1.1) or Eq. (1.6), and then apply the procedure of Sec. 2. Closed ghost loops vanish in this case, so they do not contribute to amplitudes of the fields  $\varphi$  and  $\lambda$ .

A slightly different method was used by Arnold and Yaffe [21] who used temporal  $A^0 = 0$  gauge to obtain the path integral representation. For the leading log Langevin equation (1.6) this leads to a supersymmetric action in the path integral. It is not clear, however, whether the analogous action for Eq. (1.1) would be supersymmetric. Then the Fadeev-Popov procedure was used in [21] to switch to Coulomb gauge.

## 4 Path integral representation of the Boltzmann-Langevin equation

We can now write the path integral representation of Eq. (1.1) as

$$\int [d\mathbf{A} d\widetilde{W} d\lambda d\eta d\bar{\eta}] e^{-S} \quad (4.1)$$

with the action

$$\begin{aligned} S &= \int d^4x \int_{\mathbf{v}} \left\{ \frac{T}{m_D^2} \lambda C \lambda - i\lambda \left[ (C + \mathbf{v} \cdot \mathbf{D}) \widetilde{W} \right. \right. \\ &\quad \left. \left. + \frac{d}{m_D^2} (c_1 + \mathbf{v} \cdot \mathbf{D}) \mathbf{v} \cdot \mathbf{D} \times \mathbf{B} - \mathbf{v} \cdot \mathbf{E} \right] \right\} + S_{\text{ghost}}. \end{aligned} \quad (4.2)$$

As was mentioned above, closed ghost loops vanish in this theory. In this paper we are only interested in amplitudes of the physical fields  $A$  and  $\widetilde{W}$  and of  $\lambda$ . Therefore we can ignore the ghost part of the action  $S_{\text{ghost}}$  in the following.

The vertices can be read off from the interaction Lagrangian

$$\begin{aligned}
S_{\text{int}} = & -ig f_{abc} \int_{k_1, k_2, k_3} (2\pi)^{d+1} \delta(k_1 + k_2 + k_3) \\
& \left\{ \int_{\mathbf{v}} \lambda_a(k_1, \mathbf{v}) [A_b^0(k_2) - \mathbf{v} \cdot \mathbf{A}_b(k_2)] \widetilde{W}_c(k_3, \mathbf{v}) \right. \\
& + \frac{1}{2} \frac{d}{m_D^2} \left[ \left[ -ic_1 \lambda_a^i(k_1) - k_1^j \lambda_a^{ij}(k_1) \right] \right. \\
& \times \left[ (k_2 - k_1)^n \delta^{il} + (k_3 - k_2)^i \delta^{nl} + (k_1 - k_3)^l \delta^{in} \right] \\
& + \lambda_a^{im}(k_1) \left[ \delta^{nm} P_t^{il}(\mathbf{k}_2) \mathbf{k}_2^2 - \delta^{lm} P_t^{in}(\mathbf{k}_3) \mathbf{k}_3^2 \right] \left. \right] A_b^l(k_2) A_c^n(k_3) \\
& \left. - \lambda_a(k_1) \cdot \mathbf{A}_b(k_2) A_c^0(k_3) + O(\lambda \mathbf{A}^3) \right\} \tag{4.3}
\end{aligned}$$

with

$$\int_k \equiv \int \frac{d^{d+1}k}{(2\pi)^{d+1}}. \tag{4.4}$$

Furthermore, we have introduced the 3–vector  $\lambda$  through

$$\lambda^i \equiv \int_{\mathbf{v}} v^i \lambda(\mathbf{v}), \tag{4.5}$$

and the traceless tensor

$$\lambda^{ij} \equiv \int_{\mathbf{v}} \left( v^i v^j - \frac{1}{d} \delta^{ij} \right) \lambda(\mathbf{v}), \tag{4.6}$$

which represent the  $l = 1$  and  $l = 2$  projections of  $\lambda(\mathbf{v})$ , respectively. Finally, the transverse projector is

$$P_t^{ij}(\mathbf{k}) = \delta^{ij} - \hat{k}^i \hat{k}^j. \tag{4.7}$$

In Eq. (4.3) we have not displayed the  $\lambda \mathbf{A}^3$  and  $\lambda \mathbf{A}^4$  vertices which do not play a role in the following. The only interaction in Eq. (4.3) which contains derivatives is the  $\lambda \mathbf{A}^2$  vertex. For power counting we can estimate this vertex as

$$(\lambda \mathbf{A} \mathbf{A}) \sim g \frac{c_1 |\mathbf{k}|}{m_D^2}, \tag{4.8}$$

where  $\mathbf{k}$  is a typical spatial momentum carried by one of the fields. The remaining non-derivative interaction vertices are simply of order  $g$ .

## 4.1 Propagators

Obtaining the propagators for Eq. (4.2) is tedious but straightforward. To simplify the notation it is useful to think of  $C$  and  $\mathbf{v}$  as operators acting on the space of functions on the 2-sphere. These functions are represented by bras and kets. We define  $|\mathbf{v}\rangle$  as the eigenvector of the operators  $\hat{v}^i$  ( $i = 1, \dots, d$ ) with eigenvalues  $v^i$ ,

$$\hat{v}^i |\mathbf{v}\rangle = v^i |\mathbf{v}\rangle \quad (4.9)$$

and with the normalization

$$\langle \mathbf{v} | \mathbf{v}' \rangle = \Omega \delta^{(S^{d-1})}(\mathbf{v} - \mathbf{v}') \quad (4.10)$$

Here  $\delta^{(S^{d-1})}$  is the delta-function on the  $d-1$  dimensional unit sphere, the surface area of which is denoted by  $\Omega$ . Then the unit operator is

$$1 = \int_{\mathbf{v}} |\mathbf{v}\rangle \langle \mathbf{v}|. \quad (4.11)$$

It is also convenient to introduce

$$|^\mu\rangle = \int_{\mathbf{v}} v^\mu |\mathbf{v}\rangle. \quad (4.12)$$

These are normalized such that

$$\langle^0|0\rangle = 1, \quad \langle^i|j\rangle = \frac{1}{d} \delta^{ij}. \quad (4.13)$$

The action (4.2) can then be written as

$$\begin{aligned} S = & \int d^4x \left\{ \frac{T}{m_D^2} \langle \lambda | \hat{C} | \lambda \rangle - i \langle \lambda | \left[ (\hat{C} + \hat{v} \cdot D) | \widetilde{W} \rangle \right. \right. \\ & \left. \left. + \frac{d}{m_D^2} (c_1 + \hat{\mathbf{v}} \cdot \mathbf{D}) |^i \rangle D_j F^{ji} - |^i \rangle E^i \right] \right\}. \end{aligned} \quad (4.14)$$

To determine the momentum space propagators one has to invert  $\hat{C} - i\hat{v} \cdot k$ . We denote its inverse by

$$\hat{G}(k) \equiv \left[ \hat{C} - i\hat{v} \cdot k \right]^{-1}. \quad (4.15)$$

For writing propagators involving gauge fields it is convenient to introduce

$$G^{\mu\nu} \equiv \langle^\mu | \hat{G} |^\nu \rangle \quad (4.16)$$

which is symmetric under exchange of  $\mu$  and  $\nu$ . Its spatial components are decomposed into transverse and longitudinal parts,

$$G^{ij} = P_t^{ij} G_t + \hat{k}^i \hat{k}^j G_\ell. \quad (4.17)$$

Some properties of  $\hat{G}$  and related functions are listed in Appendix A.

We give the expressions for propagators in Coulomb gauge. The propagators for general flow gauge can then be obtained by using Eq. (3.4). We denote spatial gauge fields by wavy,  $A_0$  by dashed,  $\widetilde{W}$  by full, and the Lagrange multiplier fields  $\lambda$  by dotted lines.

The  $\lambda\lambda$  propagator vanishes,

$$\lambda \bullet \dots \bullet \lambda = 0. \quad (4.18)$$

This is an immediate consequence of the invariance under the BRST transformation (2.8). Due to ghost-number conservation we have  $\langle \lambda \bar{\eta} \rangle = 0$ . Performing a BRST transformation in the path integral for  $\langle \lambda \bar{\eta} \rangle = 0$  then gives  $\langle \lambda \lambda \rangle = 0$ .

The off-diagonal propagators mixing the physical fields with  $\lambda$  are not invariant under changing sign of the momentum. Therefore we explicitly display the momentum variables,

$$A^i(k) \bullet \sim \dots \bullet \lambda(-k, \mathbf{v}) = i \langle S^i(k) | \mathbf{v}' \rangle, \quad (4.19)$$

$$A^0(k) \bullet \dots \bullet \lambda(-k, \mathbf{v}) = i \langle S^0(k) | \mathbf{v} \rangle. \quad (4.20)$$

The expressions

$$\langle S^i(k) | \equiv m_D^2 \widetilde{\Delta}(k) P_t^{ij}(\mathbf{k}) \langle^j | \hat{G}(k), \quad (4.21)$$

with

$$\widetilde{\Delta}(k) \equiv [1 + idk_0 G_t(k)]^{-1} \Delta(k), \quad (4.22)$$

$$\Delta(k) \equiv \frac{1}{\mathbf{k}^2 - im_D^2 k_0 G_t(k) [1 + idk_0 G_t(k)]^{-1}} \quad (4.23)$$

and

$$\langle S^0(k) | \equiv \frac{-i}{\mathbf{k}^2 G_\ell(k)} k^i \langle^i | \hat{G}(k) (1 - \hat{P}_0) \quad (4.24)$$

will also appear in the  $A^\mu - \widetilde{W}$  propagators below. The  $\widetilde{W} - \lambda$  propagator can be written as

$$\widetilde{W}(k, \mathbf{v}) \bullet \dots \bullet \lambda(-k, \mathbf{v}') \rangle = i \langle \mathbf{v} | \left( 1 - \hat{P}_0 - \hat{P}_1 \right) \hat{S}(k) \left( 1 - \hat{P}_0 \right) | \mathbf{v}' \rangle. \quad (4.25)$$

$\hat{P}_0$  and  $\hat{P}_1$  are the projectors onto the  $l = 0$  and  $l = 1$  sectors,

$$\hat{P}_0 \equiv |^0\rangle\langle^0|, \quad \hat{P}_1 \equiv d|^i\rangle\langle^i| \quad (4.26)$$

and

$$\begin{aligned} \hat{S}(k) &\equiv \hat{G}(k) - \frac{1}{G_\ell(k)} \hat{G}(k) |^i\rangle\langle^i| \hat{k}^i \hat{k}^j \langle^j | \hat{G}(k) \\ &\quad - \frac{1}{G_t(k)} \left[ 1 - \mathbf{k}^2 \widetilde{\Delta}(k) \right] \hat{G}(k) |^i\rangle P_t^{ij}(\mathbf{k}) \langle^j | \hat{G}(k). \end{aligned} \quad (4.27)$$

Note that all propagators which mix  $\lambda$  with the "matter" fields  $A^\mu$  and  $\widetilde{W}$  have poles only in the lower half of the complex  $k^0$  plane. As a consequence, loops which contain only such propagators vanish.

To obtain the propagators for the physical fields, one uses

$$\hat{G}(k) \hat{C} \hat{G}(-k) = \frac{1}{2} \left[ \hat{G}(k) + \hat{G}(-k) \right], \quad (4.28)$$

and

$$[G_t(k) + G_t(-k)] \widetilde{\Delta}(k) \widetilde{\Delta}(-k) = \frac{1}{m_D^2} \frac{-i}{k_0} [\Delta(k) - \Delta(-k)]. \quad (4.29)$$

After some algebra one finds that the gauge field propagators take the form

$$A^i \bullet \sim \sim \bullet A^j = T P_t^{ij} \frac{-i}{k^0} \Delta(k) + (k \rightarrow -k), \quad (4.30)$$

$$A^0 \bullet \dots \bullet A^0 = \frac{T}{m_D^2} \frac{1}{\mathbf{k}^2 G_\ell(k)} + (k \rightarrow -k). \quad (4.31)$$

Note that

$$\Delta^*(k) = \Delta(-k). \quad (4.32)$$

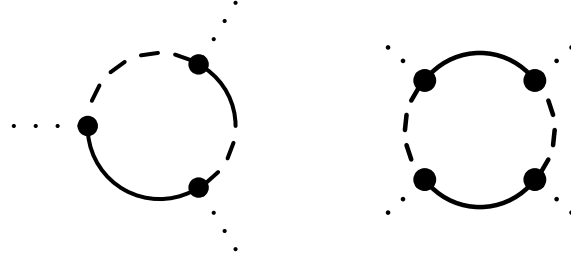


Figure 1: Examples for 1-loop diagrams which are ultraviolet divergent, and for which no counterterms are available in the action (4.2).

The off-diagonal propagators are

$$\widetilde{W} \bullet \text{---} \bullet A^i = \frac{T}{m_D^2} \langle \mathbf{v} | (1 - \hat{P}_1) | S^i(k) \rangle + (k \rightarrow -k), \quad (4.33)$$

$$\widetilde{W} \bullet \text{---} \bullet A^0 = \frac{T}{m_D^2} \langle \mathbf{v} | (1 - \hat{P}_1) | S^0(k) \rangle + (k \rightarrow -k), \quad (4.34)$$

where  $|S^\mu\rangle$  has been defined in Eqs. (4.21), (4.24) above. Finally, using again Eqs. (4.28), (4.29) one finds the  $\widetilde{W}$  propagator as

$$\widetilde{W} \bullet \text{---} \bullet \widetilde{W} = \frac{T}{m_D^2} \langle \mathbf{v} | \left(1 - \hat{P}_0 - \hat{P}_1\right) \hat{S}(k) \left(1 - \hat{P}_0 - \hat{P}_1\right) | \mathbf{v}' \rangle + (k \rightarrow -k). \quad (4.35)$$

## 5 Large momentum behavior of the propagators, 1-loop ultraviolet divergences, and renormalizability

In this section we first study the large momentum behavior of the propagators to see what kind of ultraviolet divergences can appear. The large momentum behavior of the  $A^0$  propagator, Eq. (4.31), can be easily estimated. We have  $G_\ell \sim 1/k$ , so that

$$\langle A^0 A^0 \rangle \sim \frac{1}{k}. \quad (5.1)$$

The  $\widetilde{W}$  propagator (4.35) shows the same behavior,

$$\langle \widetilde{W} \widetilde{W} \rangle \sim \frac{1}{k}. \quad (5.2)$$

Now consider the transverse gauge field propagator (4.30)

$$\langle \mathbf{A} \mathbf{A} \rangle \sim \frac{1}{k^0} [\Delta(k) - \Delta(-k)]. \quad (5.3)$$

One can write the square bracket as

$$\Delta(k) - \Delta(-k) = \frac{2im_D^2 k^0 \text{Re}G_t}{[k^2 + k^0(m_D^2 - dk^2)\text{Im}G_t]^2 + k_0^2(m_D^2 - dk^2)\text{Re}G_t^2}. \quad (5.4)$$

For  $\mathbf{k}^2 \gg m_D^2$  one can simplify the denominator,

$$\Delta(k) - \Delta(-k) \simeq \frac{1}{\mathbf{k}^4} \frac{2im_D^2 k^0 \text{Re}G_t}{[1 - dk^0 \text{Im}G_t]^2 + d^2 k_0^2 \text{Re}G_t^2}. \quad (5.5)$$

For large momenta the products  $k^0 \text{Re}G_t$  and  $k^0 \text{Im}G_t$  are at most of order unity. Thus for  $\mathbf{k}^2 \gg m_D^2$  the transverse gauge field propagator (4.30) scales like

$$\langle \mathbf{A} \mathbf{A} \rangle \sim \frac{1}{k^0 \mathbf{k}^4}. \quad (5.6)$$

It is a little puzzling that this asymptotic behavior sets in only when  $\mathbf{k}^2 \gg m_D^2$ , which is well outside the range of validity of Eq. (1.1),  $\mathbf{k}^2 \ll m_D^2$ .

A consequence of Eq. (5.6) is that the diagrams (D.2), (D.3), (D.5) in Appendix D, which contain transverse gauge field propagators, would be ultraviolet finite when computed with the propagator (4.30). The results in Appendix D are obtained by using the approximated propagators of Appendix B giving ultraviolet divergent results (see the discussion at the end of Sec. 6).

## 5.1 Renormalizability

Now we address the question whether Eq. (1.1) is a renormalizable effective theory. As we have seen above, certain propagators, like  $\langle \widetilde{W} \widetilde{W} \rangle$  and  $\langle A^0 A^0 \rangle$ , fall off only like  $1/k$  for  $k \rightarrow \infty$ . Therefore diagrams with 3 and 4 external  $\lambda$  lines, which contain only these propagators (see Fig. 5), are linearly and logarithmically divergent. The terms in the action (4.2), on the other hand, are at most quadratic in  $\lambda$ . Thus in order to renormalize these divergences one would have to introduce new terms in the action. But then the path integral (4.1) would no longer be equivalent to the Langevin equation (1.1). Thus it would not be possible to use the theory (1.1) for lattice simulations if one wants to take the continuum limit <sup>8</sup>. If one is interested in calculating corrections to the leading log Langevin equation in an expansion in  $[\log(1/g)]^{-1}$  this does not pose a problem since the divergent terms would contribute at higher orders in  $g$ .

---

<sup>8</sup> It is of course possible that these divergent contributions cancel among different diagrams. However, I do not see a reason why such a cancellation should occur.

## 6 The logarithmic approximation beyond leading order

Arnold and Yaffe have argued that the leading log Langevin equation (1.6) is also valid at next-to-leading logarithmic order (NLLO). We will now present a simple argument why this should indeed be the case.

Let us first recall the argument which takes us from Eq. (1.1) to Eq. (1.6) in the *leading* log approximation.

For the non-perturbative fields with spatial momenta of order  $g^2 T$  the collision term, which is of order  $g^2 \log(1/g) T$ , is large compared to the term containing  $\mathbf{v} \cdot \mathbf{D}$ . If one neglects the latter, the  $l = 1$  projection of Eq. (1.1) does not contain  $\widetilde{W}$  and is thus a closed equation for the gauge fields alone<sup>9</sup>, which is precisely Eq. (1.6). Similarly, the equations for different  $l$  and  $m$  components of  $\widetilde{W}$  decouple in the leading log approximation.

Now imagine continuing this approximation scheme by expanding in powers of  $L^{-1} \equiv \log(1/g)^{-1}$ . For the moment we ignore the Fourier components with  $\mathbf{k} \sim L g^2 T$ . At NLL order the  $l = 1$  projection of Eq. (1.1) contains a term which schematically looks like  $\mathbf{v} \cdot \mathbf{D} \widetilde{W}_{l=2}$ . At this order we can use the leading log approximation for  $\widetilde{W}_{l=2}$  to write

$$\mathbf{v} \cdot \mathbf{D} \widetilde{W}_{l=2} \sim \mathbf{v} \cdot \mathbf{D} C^{-1} \xi_{l=2} \sim \log(1/g)^{-1} \xi_{l=2}. \quad (6.1)$$

Thus it would appear that the correction term is suppressed by only a single power of  $L^{-1}$ . However, since the correlation functions of  $\xi$  are diagonal in the  $(l, m)$  basis (see Eq. (1.4)), one needs at least two factors of  $\xi_{l=2}$  to obtain a non-vanishing contribution. But then one also gets two factors of  $L^{-1}$ , which shows that the correction term in Eq. (6.1) would become relevant only at next-to-next-to-leading log order. Thus even at NLLO we can ignore the the  $l \geq 2$  projections of Eq. (4.2), and we can drop  $\widetilde{W}$  field from (4.2). Then we obtain the action

$$S_b = \int d^4x \left\{ \frac{T}{\gamma_b} \boldsymbol{\lambda}^2 - i \boldsymbol{\lambda} \cdot \left( \frac{1}{\gamma_b} \mathbf{D} \times \mathbf{B} - \mathbf{E} \right) \right\} \quad (6.2)$$

with

$$\gamma_b \equiv \frac{m_D^2}{dc_1}. \quad (6.3)$$

---

<sup>9</sup>For a detailed discussion see [24].

The modes with spatial momenta of order of the collision term,  $\mathbf{k} \sim g^2 LT$ , <sup>10</sup> enter the soft non-perturbative dynamics through loops. They can be treated perturbatively, where the loop expansion parameter is  $L^{-1}$ . They change the coefficients in the action which becomes

$$S = \int d^4x \left\{ \frac{T}{\gamma_b} Z_\lambda \boldsymbol{\lambda}^2 - i \boldsymbol{\lambda} \cdot \left( \frac{1}{\gamma_b} Z_B \mathbf{D} \times \mathbf{B} - Z_E \mathbf{E} \right) \right\}. \quad (6.4)$$

The  $k \sim C$  modes will also introduce higher dimensional operators in Eq. (6.4). These, however, are suppressed by powers of  $g^2 T/C \sim L^{-1}$ .

The Lagrange multiplier field  $\boldsymbol{\lambda}$  can be rescaled to bring the action back into the form (6.2),

$$\boldsymbol{\lambda} \rightarrow Z_E^{-1} \boldsymbol{\lambda}, \quad (6.5)$$

so that Eq. (6.4) becomes

$$S = \int d^4x \left\{ \frac{T}{\gamma_b} \frac{Z_\lambda}{Z_E^2} \boldsymbol{\lambda}^2 - i \boldsymbol{\lambda} \cdot \left( \frac{1}{\gamma_b} \frac{Z_B}{Z_E} \mathbf{D} \times \mathbf{B} - \mathbf{E} \right) \right\}. \quad (6.6)$$

Now we can read off the color conductivity  $\gamma$  which takes into account of the  $\mathbf{k} \sim g^2 LT$  modes from the coefficient of the second term in Eq. (6.4),

$$\gamma = \frac{Z_E}{Z_B} \gamma_b. \quad (6.7)$$

Alternatively one could read off  $\gamma$  from the first term in Eq. (6.4) because we already know that both Eq. (6.4) and Eq. (1.1) generate a thermal ensemble of magnetic scale gauge fields at temperature  $T$  [22, 25, 15] (see also Eq. (1.5)). In other words, the temperature  $T$  in Eq. (6.6) is the same temperature appearing in Eq. (1.1). Therefore we must have

$$\gamma = \frac{Z_E^2}{Z_\lambda} \gamma_b. \quad (6.8)$$

Thus the  $Z$ -factors must be related by

$$Z_\lambda = Z_E Z_B, \quad (6.9)$$

and the action contains only one unknown physical parameter  $\gamma$ . Thus in order to determine  $\gamma$  rather than to calculate the  $Z$ -factors it is sufficient to calculate one single quantity in the theories (1.1) and (1.6) and require that the results match.

---

<sup>10</sup>For simplicity we will oftentimes write  $\mathbf{k} \sim C$  instead of  $\mathbf{k} \sim g^2 LT$ .

We have seen in Sec. 5 that loops containing gauge field propagators in general receive non-trivial contributions from momenta of order  $m_D \sim gT$ . These will not be included in the calculation of  $\gamma$  in Sec. 7, i.e., the calculation in Sec. 7 is performed with an ultraviolet cutoff separating the scales  $gT$  and  $g^2T$ . Technically this is achieved in dimensional regularization by not using the propagators of Sec. 4 but the approximated expressions for  $\mathbf{k}^2 \ll m_D^2$ . These are listed in Appendix B.

## 7 Determining $\gamma$ by calculating Wilson loops

To determine the next-to-leading log color conductivity  $\gamma$  we follow Arnold and Yaffe [21] and match the results for a rectangular Wilson loop  $\mathcal{W}(t, R)$ , with spatial extent  $R$  and temporal extent  $t$ , in the theory (6.4) and in the underlying "microscopic" theory, which in our case is Eq. (1.1). The Wilson loop is defined as

$$\mathcal{W}(t, R) = d_R^{-1} \text{tr} \left\langle \text{P} \exp \left\{ ig \int dx \cdot A \right\} \right\rangle, \quad (7.1)$$

where  $\text{P}$  denotes path ordering, and the integration is along a closed contour starting at  $x^\mu = 0$ , then going a distance  $R$  in the  $z$ -direction, then a distance  $t$  in the time direction, back in the  $z$ -direction to  $z = 0$  and finally back to  $x^\mu = 0$  along the time direction. The normalization factor  $d_R^{-1}$ , where  $d_R$  is the dimension of the representation  $R$  associated with the Wilson loop, is included so that  $|\mathcal{W}| \leq 1$ .

One has to choose  $R$  such that  $R^{-1} \gg g^2 T$ , so that one can obtain perturbative contributions to  $\mathcal{W}$  (see Sec. 7.1). Furthermore, one needs  $R^{-1} \ll g^2 \log(1/g)T$ , where both theories (1.1) and (1.6) are valid. Unlike in [21] we do not consider the limit  $t \rightarrow \infty$ . We first consider Coulomb gauge and later the general flow gauge (3.3).

At lowest non-trivial order the contributions to  $\mathcal{W}$  are due to propagators connecting the loop with itself. As in [21] we ignore contributions connecting one edge with itself, these depend either only on  $t$  or only on  $R$ . In Coulomb gauge there are no diagrams which connect a space-like edge with a time-like one. Thus at second order in the fields there are two contributions,

$$\mathcal{W}^{(2)}(t, R) = \mathcal{W}_{\text{time}}^{(2)}(t, R) + \mathcal{W}_{\text{space}}^{(2)}(t, R), \quad (7.2)$$

with <sup>11</sup>

$$\mathcal{W}_{\text{time}}^{(2)}(t, R) = g^2 C_R \int_0^t dt_1 \int_0^t dt_2 \langle A^0(t_1, \mathbf{0}) A^0(t_2, R\hat{\mathbf{z}}) \rangle, \quad (7.3)$$

$$\mathcal{W}_{\text{space}}^{(2)}(t, R) = g^2 C_R \int_0^R dz_1 \int_0^R dz_2 \langle A^z(0, z_1 \hat{\mathbf{z}}) A^z(t, z_2 \hat{\mathbf{z}}) \rangle, \quad (7.4)$$

where  $C_R$  is the quadratic Casimir operator of the representation  $R$ .

## 7.1 $\mathcal{W}^{(2)}$ in the leading log Langevin equation

Calculating  $\mathcal{W}(t, R)$  from in the theory (1.6) is straightforward. The propagators are the ones for Eq. (1.1) in the limit that  $k^0 \sim g^4 T$  (modulo logarithms) and  $|\mathbf{k}| \ll C$ . The relevant expressions are listed in Appendix B.2. Here  $\gamma$  must be understood as the complete NLLO color conductivity which includes the effect of the modes with  $\mathbf{k} \sim C$ . Thus we have

$$A^0 \bullet \cdots \bullet A^0 = \frac{2T}{\gamma \mathbf{p}^2}, \quad (7.5)$$

$$A^i \sim \sim \sim A^j = T P_{\text{t}}^{ij} \frac{-i}{p^0} \frac{1}{\mathbf{p}^2 - i\gamma p^0} + (p \rightarrow -p). \quad (7.6)$$

First consider  $\mathcal{W}_{\text{time}}^{(2)}$ . The integral over  $p$  is saturated by momenta  $|\mathbf{p}| \sim R^{-1}$ , and one obtains

$$\mathcal{W}_{\text{time}}^{(2)}(t, R) = \frac{C_R g^2 T}{2\pi} \frac{t}{\gamma R}. \quad (7.7)$$

To compute  $\mathcal{W}_{\text{space}}^{(2)}$  we first perform the integration over  $z_1$  and  $z_2$ , then the  $p^0$ -integration which gives

$$\mathcal{W}_{\text{space}}^{(2)}(t, R) = -\frac{C_R g^2 T}{2\pi^2} \int_0^\infty \frac{dp}{p^2} e^{-p^2 t/\gamma} \int_{-1}^1 d\cos\theta \frac{1 - \cos^2\theta}{\cos^2\theta} [1 - \cos(pR \cos\theta)]. \quad (7.8)$$

This integral can be simplified if we choose

$$\frac{t}{\gamma} \gg R^2. \quad (7.9)$$

Then the dominant contribution is from the integration region  $p^2 \sim \gamma/t \ll R^{-2}$ . For Eq. (7.8) to be reliable we need  $p \gg g^2 T$ , i.e.,  $t/\gamma \ll (g^2 T)^{-2}$ . Since  $pR \ll 1$  the

---

<sup>11</sup>In Ref. [21] there is a sign error in the analogue of Eq. (7.3). Exponentiating Eq. (7.3) (with the correct sign) one would find that  $\mathcal{W}$  grows exponentially for  $t \rightarrow \infty$ . This error does, however, not affect the result for the color conductivity because the wrong sign it is used consistently.



Figure 2: The full  $A^0$  propagator in Coulomb gauge.

square bracket can be expanded around  $pR = 0$ , and to lowest non-trivial order in this expansion we obtain

$$\mathcal{W}_{\text{space}}^{(2)} = -\frac{C_R g^2 T}{6\sqrt{\pi}} \frac{t}{\gamma R} \left( \frac{\gamma R^2}{t} \right)^{\frac{3}{2}}. \quad (7.10)$$

Due to Eq. (7.9) this is small compared to the result for the temporal contribution (7.7).

Higher loops will receive contributions from momenta of order  $g^2 T$ , and are thus not calculable in perturbation theory. By construction, these are the same in both theories (1.1) and (1.6) and can be discarded for a matching calculation. This is achieved by using dimensional to cut off both ultraviolet and infrared divergences. With this regularization loop corrections to Eqs. (7.7) vanish. Then the leading non-trivial contribution to  $\mathcal{W}^{(2)}$  is given by Eq. (7.7) provided that

$$g^2 T \ll \frac{\gamma}{t} \ll R^{-1} \ll C. \quad (7.11)$$

## 7.2 $\mathcal{W}^{(2)}$ in the Boltzmann-Langevin equation

Now we compute  $\mathcal{W}^{(2)}$  in the theory (1.1) and match the result with Eq. (7.7) to determine the next-to-leading log color conductivity  $\gamma$ . We have seen in Sec. 7.1 that in Coulomb gauge  $\mathcal{W}^{(2)}$  is determined by the  $A^0$ -propagator. The lowest order contribution is again given Eq. (7.7) but with  $\gamma$  replaced by the 'bare' value  $\gamma_b$ . Now loop corrections to this result do not vanish, and we have to compute the 1-loop contributions to the  $A^0$ -propagator.

First let us note that the  $AA$  self-energy is zero. Every interaction vertex involves one  $\lambda$  field. Thus each propagator in the loop would be a propagator which mixes  $\lambda$  with a physical field. Then all propagators in the loop have singularities only in the lower half of the complex  $k^0$  plane when  $k$  is the loop momentum. Consequently, the  $k^0$ -integration contour can be moved to  $i\infty$ , and the integral vanishes. One can also understand this as a result of the invariance of the effective action  $\Gamma$ , the generating functional of 1-particle irreducible Green functions, under the BRST-transformation (2.8).  $\Gamma$  is invariant because the transformation (2.8) is linear. A term

$\frac{1}{2}\varphi^i\Pi^{ij}\varphi^j$  in  $\Gamma$  would transform into  $\varphi^i\Pi^{ij}\bar{\epsilon}\eta^j$ , and there is no other term which transforms into this, so it must vanish.

Thus the full  $A^0$ -propagator only receives contributions from the  $\lambda\lambda$ - and  $A^0\lambda$ -selfenergies (see Fig. 2). For small momenta  $A^0$  decouples from the  $l \geq 2$  components of  $\lambda$  (see Eq. (B.15)), and we only have to consider the selfenergies for the  $l = 1$  or vector part  $\lambda^i = \langle^i|\lambda\rangle$ . The diagrams for  $\Pi_{\lambda\lambda}$  are depicted in Appendix D. For loop momenta with  $k^0 \sim C^3/m_D^2$ ,  $\mathbf{k} \sim C$  they contribute

$$\Pi_{\lambda\lambda} \sim g^2 TC^{-1} \times \frac{TC}{m_D^2} \sim \log(1/g)^{-1} \times \frac{TC}{m_D^2}. \quad (7.12)$$

This has to be compared with the coefficient of the  $\lambda\lambda$ -term in the action (4.14) which is of order  $TC/m_D^2$ . Therefore  $\Pi_{\lambda\lambda}$  yields a contribution to the  $A^0$ -propagator which is of next-to-leading order in  $\log(1/g)^{-1}$ . In addition to the diagrams in Appendix D there are diagrams involving the  $\lambda A^0 \widetilde{W}$  vertex. Using the estimates (B.5), (B.12) one easily sees that these are suppressed compared to Eq. (7.12) by powers of  $g$ .

The contributions due to loop momenta  $k^0 \sim \mathbf{k} \sim C$  are easily estimated since then all propagators are of the same order of magnitude (see Eq. (B.5)). One finds

$$\Pi_{\lambda\lambda} \Big|_{\text{loop frequency} \sim C} \sim \frac{g^2 TC}{m_D^2} \times \frac{TC}{m_D^2} \sim g^2 \log(1/g) \times \frac{TC}{m_D^2}, \quad (7.13)$$

which is suppressed compared to (7.12) by two powers of  $g$ . Thus, unlike for the **AA**-selfenergy to be discussed in Sec. 8, the loop frequencies of order  $C$  can be neglected here.

Now consider the  $\lambda A^0$ -selfenergy. For the diagrams listed in Appendix D we estimate  $\Pi_{\lambda A^0} \sim g^2 T$  for loop momenta with  $k^0 \sim C^3/m_D^2$ . For loop momenta with  $k^0 \sim C$  we find  $\Pi_{\lambda A^0} \sim g^4 T$  modulo  $\log(1/g)$ . Again the contributions which contain the  $\lambda A^0 \widetilde{W}$ -vertex are suppressed.

Thus we can use the simplified form of the propagators from Sec. B.2 to compute the loop integrals. For the external lines we can use the approximations in Sec. B.2.2. In Coulomb gauge we find that the  $A^0$  propagator for  $p^0 \ll C^3/m_D^2$  and  $|\mathbf{p}| \ll C$  is given by

$$\begin{aligned} \bullet - \text{---} \text{---} \bullet &= \bullet - \text{---} \text{---} \bullet + -\frac{p^i p^j}{\mathbf{p}^4} \times \dots \text{---} \text{---} \bullet + 4d \frac{TC_1}{m_D^2} \frac{p^i}{\mathbf{p}^4} \times \dots \text{---} \text{---} \bullet \\ &= \frac{2T}{\gamma_b \mathbf{p}^2} + \frac{1}{\mathbf{p}^2} \Pi_{\lambda\lambda}(0) - \frac{4dc_1 T}{m_D^2} \frac{p^i}{\mathbf{p}^4} \frac{\partial \Pi_{\lambda A^0}^i}{\partial p^j} \Big|_{p=0} p^j \end{aligned} \quad (7.14)$$

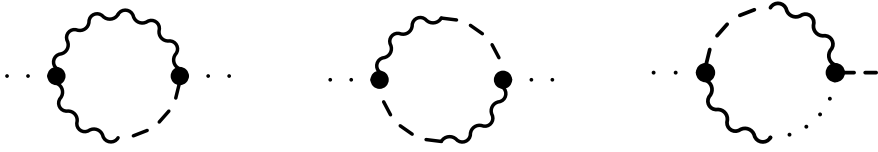


Figure 3: Examples for additional contributions to the  $\Pi_{\lambda\lambda}$  and  $\Pi_{\lambda A^0}$  self-energies in the flow gauge (3.3) with  $\kappa \neq 0$ .

$$\begin{aligned}
&= \frac{2T}{\gamma_b \mathbf{p}^2} + 2d \frac{Ng^2 T^2}{m_D^2 \mathbf{p}^2} \int_{\mathbf{k}} \left\{ \frac{1}{\mathbf{k}^2} P_t^{lm}(\mathbf{k}) \langle^0 | \hat{v}^k \hat{v}^l \hat{G}(0, \mathbf{k}) \hat{v}^k \hat{v}^m |^0 \rangle \right. \\
&\quad \left. + (d-1)c_1^2 \frac{G_t(0, \mathbf{k})}{\mathbf{k}^4} + 4 \frac{d-1}{d} \frac{c_1}{\mathbf{k}^4} [1 - dc_1 G_t(0, \mathbf{k})] \right\}.
\end{aligned}$$

Comparing this with the corresponding expression for the NLLO Langevin equation (7.5) we find

$$\begin{aligned}
\frac{1}{\gamma} &= \frac{1}{\gamma_b} + \frac{dNg^2 T}{m_D^2} \int_{\mathbf{k}} \left\{ \frac{1}{\mathbf{k}^2} P_t^{lm}(\mathbf{k}) \langle^0 | \hat{v}^k \hat{v}^l \hat{G}(0, \mathbf{k}) \hat{v}^k \hat{v}^m |^0 \rangle \right. \\
&\quad \left. + (d-1)c_1^2 \frac{G_t(0, \mathbf{k})}{\mathbf{k}^4} + 4 \frac{d-1}{d} \frac{c_1}{\mathbf{k}^4} [1 - dc_1 G_t(0, \mathbf{k})] \right\}. \quad (7.15)
\end{aligned}$$

for the NLLO color conductivity  $\gamma$  in agreement with the result of Arnold and Yaffe [21]<sup>12</sup>. We have not checked the numerical evaluation of  $\gamma$  performed in [21].

### 7.3 Gauge fixing dependence

In this section we address the question whether the above result for the Wilson loop and thus for the color conductivity depends on our gauge choice for the theory (1.1). Consider the gauge (3.3) for  $\kappa \neq 0$ . One could leave the parametric size of  $\kappa$  arbitrary, but for the purpose of power counting it is a lot more convenient to adopt a natural choice in terms of some scale which is already present in Eq. (1.1).

In the leading log theory (1.6) there would be only one natural choice. The characteristic frequency of the transverse gauge fields is  $k^0 \sim \mathbf{k}^2/\gamma$ , which can be seen from Eq. (7.6). In Coulomb gauge the  $A^0$ -propagator, Eq. (7.5), is frequency-independent.

<sup>12</sup> Arnold and Yaffe [21] write their results in terms of  $\sigma_{\mathbf{k}} = \bar{\sigma}_T^{(0)}(\mathbf{k})$ , which is related to our notation by  $\sigma_{\mathbf{k}} = \bar{\sigma}_T^{(0)}(\mathbf{k}) = m_D^2 G_t(0, \mathbf{k})$ . Furthermore, their  $\gamma_1$  is the same as our  $c_1$ .

By choosing  $\kappa \sim \gamma$  one would make the characteristic frequencies of all gauge field components equal at tree level.

For Eq. (1.1) there is an additional option. Consider the  $A^0$  propagator in Eq. (4.31).  $G_\ell(k)$  has discontinuities for  $k^0$  of order of the collision term  $C$ , and so does the  $A^0$ -propagator. When  $\mathbf{k} \sim C$ , the characteristic frequency of the transverse gauge fields is of order  $C$  as well. Thus one would naturally use  $\kappa \sim C$ . This case turns out to be very easy to analyze. As long as  $k^0 \sim g^4 T$  (modulo logs) all propagators involving  $A^0$  are approximately the same as in Coulomb gauge, and we do not have to recalculate any of the diagrams in Appendix D. Furthermore, even for  $k^0 \sim C$ ,  $A^0$  is of the same order of magnitude as in Coulomb gauge. Therefore the suppression of the integration region  $k^0 \sim C$  found in Sec. 7.2 persists. There are additional diagrams contributing to the  $\Pi_{\lambda\lambda}$  and  $\Pi_{\lambda A^0}$  self-energies due to the mixing of  $A^0$  and  $\mathbf{A}$ , see Fig. 3. Using the estimates of Appendix B one easily finds that all these contributions are suppressed by powers of  $g$ . There are also contributions to the 1-loop  $A^0$ -propagator of the form

$$\langle A^0 A^0 \rangle_{1\text{-loop}} \sim \langle A^0 \mathbf{A}_\ell \rangle \Pi_{\mathbf{A}\lambda} \langle \lambda A^0 \rangle. \quad (7.16)$$

The longitudinal gauge field  $\mathbf{A}_\ell$  is of the same order of magnitude as  $A_{\text{Coul}}^0$  when  $\mathbf{k} \sim C$ , and of order  $\kappa/|\mathbf{k}| \sim C/(g^2 T)$  times  $A_{\text{Coul}}^0$  when  $\mathbf{k} \sim g^2 T$ . Therefore  $\langle A^0 \mathbf{A}_\ell \rangle \lesssim \langle A^0 A^0 \rangle$ . The self-energy  $\Pi_{\mathbf{A}\lambda}$  is estimated in Sec. 8 as  $(g^2 T)^3/m_D^2$  modulo logs. Finally, from Eq. (B.18)  $\langle \lambda A^0 \rangle \sim (g^2 T)^{-1}$ , so that

$$\langle A^0 \mathbf{A} \rangle \Pi_{\mathbf{A}\lambda} \langle \lambda A^0 \rangle \lesssim \frac{(g^2 T)^2}{m_D^2} \langle A^0 A^0 \rangle \quad (7.17)$$

which is strongly suppressed compared to the tree level result for  $\langle A^0 A^0 \rangle$ . Thus we conclude that the result for the Wilson loop in the theory (1.1) is not changed if one uses the flow gauge with  $\kappa \sim C$  instead of Coulomb gauge <sup>13</sup>.

## 8 Transverse gauge field propagator at one loop

We have seen that the NLLO color conductivity can be obtained by considering only the  $A^0$ -propagator which gives the dominant contribution to the Wilson loop of Sec. 7. By simple power counting we have found that the contribution from loop momenta  $k$

<sup>13</sup>Things become more complicated for  $\kappa \sim \gamma$ . In this case Eq. (7.16) would contribute to the NLLO result for the Wilson loop. Furthermore, one would have to take into account not only self-energy corrections to the  $A^0$ -propagator but also vertex corrections.

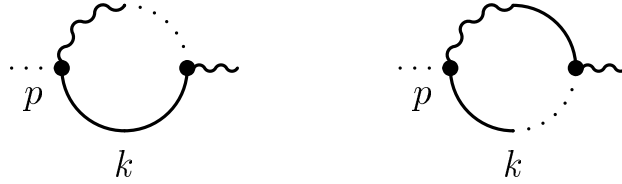


Figure 4: One loop contributions to the  $\mathbf{A}\text{-}\lambda$  self-energy which receive equal contributions from loop momenta with  $k^0$  of order  $g^2T$  and of order  $g^4T$ .

with <sup>14</sup>  $k^0 \sim g^2T$  is suppressed by *powers* of  $g$ . Thus it appears that the dynamics associated with this frequency scale (see Ref. [15]) is irrelevant to the soft gauge field dynamics. From the discussion in Sec. 6 it should be clear that one could have chosen another quantity for the matching calculation which receives contributions from spatial gauge fields as well.

In this section we will try to see whether the spatial gauge field propagator is affected by loop momenta with  $k^0 \sim g^2T$ , when external momenta are of order  $\mathbf{p} \sim g^2T$ ,  $p^0 \sim g^4T$ . It cannot be calculated perturbatively, but one can calculate the contribution from loop momenta large compared to  $g^2T$ , which is the philosophy of Ref. [18].

As we discussed in Sec. 7.2 the  $AA$  self-energy vanishes. Thus we only obtain contributions which contain the  $\lambda\mathbf{A}$  and  $\lambda\lambda$  self-energies. The latter has already been considered in Sec. 6. Consider now the contribution of the  $\lambda\mathbf{A}$  self-energy depicted in Fig. 14 and use the estimates in Eq. (B.12). The  $\mathbf{A}\lambda$  propagator is of order  $C^{-1}$  and  $m_D^2/C^3$  for  $k^0 \sim C$  and  $k^0 \sim C^3/m_D^2$ , respectively. Therefore for both these frequency scales the product  $k^0\langle\mathbf{A}\lambda\rangle$  is of the same order of magnitude  $k^0\langle\mathbf{A}\lambda\rangle \sim 1$ . The other propagator in the loop is of the same order for both frequencies,  $\langle\widetilde{WW}\rangle \sim T/(m_D^2 C)$ . The integration over 3-momenta is of order  $C^3$ , and there is a factor  $g^2$  from the vertices. Thus we obtain  $\Pi_{\mathbf{A}\lambda} \sim g^2 T C^2/m_D^2$ . This would give a contribution to the  $\mathbf{AA}$  propagator of order (cf. Eq. (B.18))

$$\langle\mathbf{AA}\rangle_{1\text{-loop}}(p) \sim \langle\mathbf{AA}\rangle \Pi_{\mathbf{A}\lambda} \langle\lambda\mathbf{A}\rangle \sim \frac{C}{g^2 T} \langle\mathbf{AA}\rangle \quad (8.1)$$

for  $\mathbf{p} \sim g^2T$ ,  $p^0 \sim C(g^2T)^2/m_D^2$ . This would mean that the 1-loop contribution is larger than the tree level by one power of  $\log(1/g)$ . However, we would expect that

---

<sup>14</sup>In this section we ignore  $\log(1/g)$  in the order of magnitude estimates, so that, e.g., the collision term  $C$  is estimated as  $C \sim g^2T$ .

$\Pi_{\mathbf{A}\lambda}(p)$  vanishes for  $p \rightarrow 0$ , and that one can expand

$$\Pi_{\mathbf{A}\lambda}(p) \sim \mathbf{p}^2 \Pi'_{\mathbf{A}\lambda} + \dots$$

Since we consider loop momenta  $k$  with  $\mathbf{k} \sim C$ ,  $\Pi'$  is of order  $\Pi/C^2$ . This would give the estimate

$$\langle \mathbf{A}\mathbf{A} \rangle_{\text{1-loop}}(p) \sim \frac{g^2 T}{C} \langle \mathbf{A}\mathbf{A} \rangle. \quad (8.2)$$

In other words, the diagram in Fig. 14 would contribute at next-to-leading logarithmic order. This is puzzling since the next-to-leading order color conductivity  $\gamma$  which was calculated from the  $A_0$  propagator alone does not receive such contributions. It was argued in Sec. 6, based on the fact that Eq. (1.1) generates the same gauge field thermodynamics as Eq. (1.6), that it is sufficient to perform a matching calculation of one single object to obtain  $\gamma$ . Now it appears that it depends on the choice of this object whether one obtains contribution from the frequency scale  $k^0 \sim C$  or not.

It is of course possible that there is a cancellation between various diagrams contributing to the  $\mathbf{A}\lambda$  self-energy so that the contribution discussed above come with a vanishing coefficient, but I do not see a reason for such a cancellation to occur.

## 9 Summary and discussion

We have found that the Boltzmann-Langevin equation (1.1) is not renormalizable by power counting. There are divergent 1-loop diagrams for which the action (4.2) contains no counterterms. Introducing the necessary counterterms would invalidate the equivalence of the path integral (4.1) and the Boltzmann-Langevin equation (1.1). The divergences appear in diagrams with  $A^0$  and  $\widetilde{W}$  propagators, which for large momenta  $k$  fall off only like  $1/k$ . One should emphasize that these divergences are *not* related to the ones in classical Yang-Mills or in the hard thermal loop effective theory discussed previously [14]. Furthermore, they do not affect the next-to-leading log order (NLLO) calculations.

We have confirmed Arnold and Yaffe's result for the NLLO color conductivity  $\gamma$  by matching the results for Wilson loops obtained from Eq. (1.1) and Eq. (1.6) using Coulomb gauge. We have checked the gauge fixing independence in a certain class of flow gauges. The dominant contribution is due to the 1-loop  $A^0$ -propagator, which turned out to be unaffected by loop momenta with  $k^0 \gg g^4 T [\log(1/g)]^3$ .

The gauge field propagator in the theory (1.1) has a non-trivial analytic structure for momenta of order  $gT$ , which lie outside the range of validity of (1.1). The calculation of the NLLO color conductivity is performed with an ultraviolet cutoff  $\mu$ ,  $g^2T \ll \mu \ll gT$ . The proof that Eq. (1.1) correctly reproduces the thermodynamics of  $\mathbf{k} \sim g^2T$  Yang-Mills fields [15] does, however, not assume the presence of such a cutoff which could be a reason for being concerned.

Finally, we have found that, somewhat surprisingly, the spatial gauge field propagator for momenta of order  $g^2T$ , unlike the  $A^0$ -propagator, *does* receive NLLO corrections from loop momenta with  $k^0 \sim g^2T \log(1/g)$ .

**Acknowledgments.** I would like to thank Poul H. Damgaard, Edwin Laermann, Kari Rummukainen and Daniel Zwanziger for useful discussions. This work was supported by the DFG, grant FOR 339/2-1.

## A Properties of $\hat{G}$ and related functions

$\hat{G}$ , defined in Eq. (4.15), is symmetric since it is the inverse of a symmetric operator,

$$\langle \mathbf{v}_1 | \hat{G}(k) | \mathbf{v}_2 \rangle = \langle \mathbf{v}_2 | \hat{G}(k) | \mathbf{v}_1 \rangle. \quad (\text{A.1})$$

Furthermore,

$$\hat{G}(-k) = \hat{G}^*(k). \quad (\text{A.2})$$

Now multiply

$$[\hat{C} - i\hat{v} \cdot k] \hat{G}(k) = 1 \quad (\text{A.3})$$

by  $\langle^0|$  from the left. The collision term drops out since its  $l = 0$  eigenvalue vanishes,

$$-i\langle^0| \hat{v} \cdot k \hat{G}(k) = \langle^0|. \quad (\text{A.4})$$

Now we use

$$\begin{aligned} \langle^0| \hat{v}^\mu &= \int_{\mathbf{v}} \langle \mathbf{v} | \hat{v}^\mu = \int_{\mathbf{v}} v^\mu \langle \mathbf{v} | \\ &= \langle^\mu| \end{aligned} \quad (\text{A.5})$$

which gives the identity

$$k^i \langle^i | \hat{G}(k) = -i\langle^0| + k^0 \langle^0 | \hat{G}(k). \quad (\text{A.6})$$

From this we obtain the following relations

$$G_\ell = \frac{k^0}{\mathbf{k}^2} (k^0 G^{00} - i) \quad (\text{A.7})$$

$$k^i G^{0i} = k^0 G^{00} - i \quad (\text{A.8})$$

and

$$G^{00} = \frac{1}{k^0} \left( \frac{\mathbf{k}^2}{k^0} G_\ell + i \right) \quad (\text{A.9})$$

$$k^i G^{0i} = \frac{\mathbf{k}^2}{k^0} G_\ell \quad (\text{A.10})$$

When  $k^0 \ll |\mathbf{k}|$  we can approximate  $G^{0i}(k)$  by

$$G^{0i}(0, \mathbf{k}) = -i \frac{k^i}{\mathbf{k}^2}. \quad (\text{A.11})$$

The following matrix elements are needed to obtain the results in Appendix D

$$\langle^{ij} | \hat{G}(0, \mathbf{k}) |^l \rangle = \frac{i}{\mathbf{k}^2} \left[ c_1 G_t(0, \mathbf{k}) - \frac{1}{d} \right] \left[ k^i P_t^{jl}(\mathbf{k}) + k^j P_t^{il}(\mathbf{k}) \right], \quad (\text{A.12})$$

$$k^i k^j \langle^{ij} | \hat{G}(0, \mathbf{k}) |^0 \rangle = c_1 - \frac{1}{d} \mathbf{k}^2 G^{00}(0, \mathbf{k}). \quad (\text{A.13})$$

## B Approximated expressions and power counting for the propagators

As discussed at the end of Sec. 6 we will not use the propagators of Sec. 4 to compute the NLLO color conductivity, but instead the approximated expressions for momenta small compared to  $m_D$ , which are much simpler. We have to consider two cases. The first is  $k^0, \mathbf{k} \sim C$ . These are the characteristic momenta for the  $\tilde{W}$  fields which perform damped oscillations in such a way that the color current vanishes (see [15]). The second case is  $k^0 \ll C$  for the characteristic frequencies of the gauge fields  $k^0 \sim g^4 T$  (modulo logarithms of  $g$ ). There we have to distinguish  $\mathbf{k} \sim C$  and  $\mathbf{k} \ll C$ .

### B.1 $k^0 \sim \mathbf{k} \sim C$

When  $k_0$  is of order  $C$  we have  $k_0 G_t \sim 1$ . Then one can neglect  $\mathbf{k}^2$  in  $\Delta(k)$ , Eq. (4.23),

$$\Delta(k) = \frac{1}{m_D^2} \left[ \frac{i}{k_0} \frac{1}{G_t} - d \right] \times (1 + O(g^2)) \quad (\text{B.1})$$

so that

$$\bullet\sim\sim\sim\bullet = \frac{T}{m_D^2} P_t^{ij} \left[ \frac{1}{k_0^2 G_t(k)} + (k \rightarrow -k) \right] \times (1 + O(g^2)). \quad (\text{B.2})$$

Furthermore,

$$|S^i\rangle = P_t^{ij} \frac{i}{k^0 G_t} \hat{G}^j \times (1 + O(g^2)) \quad (\text{B.3})$$

and

$$\hat{S} \simeq \hat{G} - i \frac{i}{k^0} \hat{P}_0 - G_\ell^{-1} \hat{G}^i \hat{k}^i \hat{k}^j \langle^j | \hat{G} - G_t^{-1} |^i \rangle P_t^{ij} \langle^j | \hat{G}. \quad (\text{B.4})$$

To estimate loop diagrams we need order of magnitude estimates for the various propagators. From the above expressions one finds

$$\begin{aligned} \langle A^\mu \lambda \rangle, \langle \widetilde{W} \lambda \rangle &\sim C^{-1} \\ \langle A^\mu A^\nu \rangle, \langle A^\mu \widetilde{W} \rangle, \langle \widetilde{W} \widetilde{W} \rangle &\sim T m_D^{-2} C^{-1} \sim L^{-1} g^{-4} T^{-2} \quad (k_0, |\mathbf{k}| \sim C). \end{aligned} \quad (\text{B.5})$$

## B.2 $k^0 \ll C$

When the frequency  $k^0$  is small compared to  $C$  the gauge field propagators are the same as in Ref. [21]. We can approximate

$$\Delta \simeq \Delta_0 \equiv \frac{1}{\mathbf{k}^2 - i m_D^2 k_0 G_t(0, \mathbf{k})} \quad (k_0 \sim g^4 T) \quad (\text{B.6})$$

$$|S^i\rangle = m_D^2 P_t^{ij} \Delta_0 \hat{G}(0, \mathbf{k}) |^j \rangle \quad (k_0 \sim g^4 T) \quad (\text{B.7})$$

$$\langle S^0(k) | = \langle^0 | \hat{G}_0(\mathbf{k}) (1 - \hat{P}_0) \quad (\text{B.8})$$

$$\bullet\cdots\bullet = 2 \frac{T}{m_D^2} G^{00}(0, \mathbf{k}) \times (1 + O(g^2)) \quad (k_0 \sim g^4 T) \quad (\text{B.9})$$

$$\begin{aligned} \langle \widetilde{W}(k, \mathbf{v}) A_0(k') \rangle &= \\ (2\pi)^{d+1} \delta(k + k') \frac{T}{m_D^2} \langle \mathbf{v} | \left( 1 - \hat{P}_0 - \hat{P}_1 \right) \left[ \hat{G}(0, \mathbf{k}) + \hat{G}(0, -\mathbf{k}) \right] |^0 \rangle & \quad (\text{B.10}) \end{aligned}$$

$$\hat{S}(k) = \hat{G}_0(\mathbf{k}) - \left( \hat{G}_0 \hat{P}_0 + \hat{P}_0 \hat{G}_0 \right) + G_0^{00} \hat{P}_0 + i m_D^2 k_0 \Delta_0 \hat{G}_0 |^i \rangle P_t^{ij} \langle^j | \hat{G}_0 \quad (\text{B.11})$$

### B.2.1 $k_0 \sim C^3/m_D^2$ and $\mathbf{k} \sim C$

For these momenta the propagators are of order

$$\begin{aligned}
\langle \mathbf{A} \lambda \rangle &\sim m_D^2 C^{-3} \\
\langle A^0 \lambda \rangle, \langle \widetilde{W} \lambda \rangle &\sim C^{-1} \\
\langle \mathbf{A} \mathbf{A} \rangle &\sim T m_D^2 C^{-5} \sim L^{-5} g^{-8} T^{-2} \\
\langle \mathbf{A} \widetilde{W} \rangle &\sim T C^{-3} \sim L^{-3} g^{-6} T^{-2} \\
\langle A^0 A^0 \rangle, \langle A^0 \widetilde{W} \rangle, \langle \widetilde{W} \widetilde{W} \rangle &\sim T m_D^{-2} C^{-1} \sim L^{-1} g^{-4} T^{-2}.
\end{aligned} \tag{B.12}$$

### B.2.2 $\mathbf{k} \sim g^2 T$

When  $\mathbf{k}$  is small compared to  $C$ , the propagators for the gauge fields become the same as in the leading log effective theory (1.6). We need the expansion of  $\hat{G}(0, \mathbf{k})$  for  $|\mathbf{k}| \ll C$

$$\begin{aligned}
\hat{G}(0, \mathbf{k}) &= \frac{d}{c_1 \mathbf{k}^2} (c_1 - i \hat{\mathbf{v}} \cdot \mathbf{k}) \hat{P}_0 (c_1 - i \hat{\mathbf{v}} \cdot \mathbf{k}) + (1 - \hat{P}_0) \hat{C}^{-1} (1 - \hat{P}_0) \\
&\quad - \frac{d}{c_2 \mathbf{k}^2} \left[ \hat{P}_0 (\hat{\mathbf{v}} \cdot \mathbf{k})^2 + (\hat{\mathbf{v}} \cdot \mathbf{k})^2 \hat{P}_0 \right] + \frac{d^2}{c_2 \mathbf{k}^4} \hat{P}_0 (\hat{\mathbf{v}} \cdot \mathbf{k})^4 \hat{P}_0 + O(\mathbf{k}/C^2).
\end{aligned} \tag{B.13}$$

In particular,

$$\hat{G}(0, \mathbf{k})|^0 \rangle = \frac{d}{\mathbf{k}^2} (c_1 - i \hat{\mathbf{v}} \cdot \mathbf{k})|^0 \rangle + O(C^{-1}), \tag{B.14}$$

$$\langle S^0(k) | = -id \frac{k^i}{\mathbf{k}^2} \langle^i | + O(C^{-1}), \tag{B.15}$$

$$G^{00}(0, \mathbf{k}) = \frac{dc_1}{\mathbf{k}^2} + O(C^{-1}), \tag{B.16}$$

and

$$G_t(0) = \frac{1}{dc_1}. \tag{B.17}$$

The propagators are of order

$$\begin{aligned}
\langle \mathbf{A} \lambda \rangle &\sim m_D^2 c_1^{-1} (g^2 T)^{-2} \\
\langle A^0 \lambda \rangle &\sim (g^2 T)^{-1}
\end{aligned}$$

$$\begin{aligned}
\langle \mathbf{A} \mathbf{A} \rangle &\sim \frac{T m_D^2}{C(g^2 T)^4} \\
\langle A^0 A^0 \rangle &\sim L g^{-4} T^{-2} \sim \frac{T c_1}{m_D^2 (g^2 T)^2} \\
|S^i\rangle &\sim L^{-1} g^{-6} T^{-2} \\
\langle A^0 \widetilde{W} \rangle &\sim L^0 g^{-4} T^{-2} \sim \frac{T}{m_D^2 c_1} \\
\langle \widetilde{W} \widetilde{W} \rangle &\sim \frac{T}{m_D^2 c_1} \quad \left( k_0 \sim \frac{C(g^2 T)^2}{m_D^2}, \mathbf{k} \sim g^2 T \right). \tag{B.18}
\end{aligned}$$

## C Frequency integrals

For the frequency integration it is convenient to write  $\Delta_0$ , which is defined in Eq. (B.6), as

$$\Delta_0(k) = \frac{i\Gamma_{\mathbf{k}}}{\mathbf{k}^2} \frac{1}{k^0 + i\Gamma_{\mathbf{k}}}, \tag{C.1}$$

where

$$\Gamma_{\mathbf{k}} \equiv \frac{\mathbf{k}^2}{m_D^2 G_t(0, \mathbf{k})}. \tag{C.2}$$

The frequency integrals for the diagrams in Appendix D are

$$\int_{k^0} \frac{1}{k^0} [\Delta_0(k) - \Delta_0(-k)] = \frac{i}{\mathbf{k}^2}, \tag{C.3}$$

$$\int_{k^0} \Delta_0(k) \Delta_0(-k) = \frac{1}{2m_D^2} \frac{1}{\mathbf{k}^2 G_t(0, \mathbf{k})}, \tag{C.4}$$

$$\int_{k^0} \frac{1}{k^2} [\Delta_0(k) - \Delta_0(-k)]^2 = -m_D^2 \frac{G_t(0, \mathbf{k})}{\mathbf{k}^6}. \tag{C.5}$$

We also need frequency integrals with external momentum  $p^\mu = (0, \mathbf{p})$ ,

$$\int_{k^0} \Delta_0(k) \Delta_0(p - k) = \frac{1}{m_D^2} \frac{1}{\mathbf{k}^2 G_t(0, \mathbf{p} - \mathbf{k}) + (\mathbf{p} - \mathbf{k})^2 G_t(0, \mathbf{k})}, \tag{C.6}$$

$$\begin{aligned}
\int_{k^0} \Delta_0(k) \frac{1}{k^0} [\Delta_0(k - p) - \Delta_0(p - k)] \\
= \frac{i G_t(0, \mathbf{p} - \mathbf{k})}{(\mathbf{p} - \mathbf{k})^2 [\mathbf{k}^2 G_t(0, \mathbf{p} - \mathbf{k}) + (\mathbf{p} - \mathbf{k})^2 G_t(0, \mathbf{k})]}, \tag{C.7}
\end{aligned}$$

$$\int_{k^0} \frac{1}{k^0} [\Delta_0(k - p) - \Delta_0(p - k)] = \frac{i}{(\mathbf{p} - \mathbf{k})^2}. \tag{C.8}$$

## D One loop results

Here we list the Coulomb gauge results for the diagrams for the  $\lambda \lambda$  and  $A^0 \lambda$ -selfenergies in the limit of small external momenta  $p$ .

One needs the expansion of  $P_t^{ij}(\mathbf{k} - \mathbf{p})$ , where  $\mathbf{k}$  is the loop momentum, for small  $\mathbf{p}$ ,

$$P_t^{ij}(\mathbf{k} - \mathbf{p}) = P_t^{ij}(\mathbf{k}) + \frac{p^l}{\mathbf{k}^2} \left[ k^i P_t^{jl}(\mathbf{k}) + k^j P_t^{il}(\mathbf{k}) \right] + O(\mathbf{p}^2/\mathbf{k}^2). \quad (\text{D.1})$$

For  $p \rightarrow 0$  the  $\lambda \lambda$ -selfenergy becomes  $\Pi_{\lambda\lambda}(p) \rightarrow \delta^{ij} \Pi_{\lambda\lambda}(0)$ . The diagrams contributing to  $-\Pi_{\lambda\lambda}(0)$  are

$$\text{Diagram} = \frac{Ng^2 T^2}{m_D^2} d(d-1) \int_{\mathbf{k}} \frac{\left( c_1 G_t(0, \mathbf{k}) - \frac{1}{d} \right)^2}{\mathbf{k}^4 G_t(0, \mathbf{k})}, \quad (\text{D.2})$$

$$\text{Diagram} = \frac{Ng^2 T^2}{m_D^2} \int_{\mathbf{k}} \left\{ -\frac{2d}{\mathbf{k}^2} P_t^{lm} \langle^{kl} | \hat{G}(0, \mathbf{k}) |^{km} \rangle - d(d-1) \frac{\left( c_1 G_t(0, \mathbf{k}) - \frac{1}{d} \right)^2}{\mathbf{k}^4 G_t(0, \mathbf{k})} \right\}, \quad (\text{D.3})$$

$$\text{Diagram} = -2c_1 d(d-1) \frac{Ng^2 T^2}{m_D^2} \int_{\mathbf{k}} \frac{G_t(0, \mathbf{k})}{\mathbf{k}^4}, \quad (\text{D.4})$$

$$\text{Diagram} = -\frac{2(d-1)}{d} \frac{Ng^2 T^2}{m_D^2} \int_{\mathbf{k}} \frac{G^{00}(0, \mathbf{k})}{\mathbf{k}^2}, \quad (\text{D.5})$$

$$\text{Diagram} = 2 \frac{Ng^2 T^2}{m_D^2} \int_{\mathbf{k}} \frac{1}{\mathbf{k}^4} \left( c_1 - \frac{1}{d} \mathbf{k}^2 G^{00}(0, \mathbf{k}) \right), \quad (\text{D.6})$$

$$\text{Diagram} = 0. \quad (\text{D.7})$$

Note that the diagram (D.6) enters  $\Pi_{\lambda\lambda}$  with an additional factor 2 because the reflected diagram gives the same contribution.

Arnold and Yaffe [21] write their results in terms of a different matrix element than the one Eq. (D.3). Ours is related to theirs by

$$P_t^{lm} \langle^{kl} | \hat{G}(0, \mathbf{k}) |^{km} \rangle = P_t^{lm} \langle^0 | \hat{v}^k \hat{v}^l \hat{G}(0, \mathbf{k}) \hat{v}^k \hat{v}^m |^0 \rangle + \frac{2c_1}{d\mathbf{k}^2} - \frac{d+1}{d^2} G^{00}(0, \mathbf{k}). \quad (\text{D.8})$$

With this relation the sum of Eqs. (D.2)–(D.6) gives

$$\Pi_{\lambda\lambda}(0) = 2d \frac{Ng^2 T^2}{m_D^2} \int_{\mathbf{k}} \left\{ \frac{1}{\mathbf{k}^2} P_t^{lm}(\mathbf{k}) \langle^0 | \hat{v}^k \hat{v}^l \hat{G}(0, \mathbf{k}) \hat{v}^k \hat{v}^m |^0 \rangle + (d-1) c_1^2 \frac{G_t(0, \mathbf{k})}{\mathbf{k}^4} \right\}. \quad (\text{D.9})$$

The  $\lambda A^0$ -selfenergy  $\Pi_{\lambda A^0}^i(p)$  vanishes for  $p = 0$ . Expanding around  $p = 0$  the lowest order contribution in  $\mathbf{p}$  is given by the diagrams

$$\text{Diagram: } \dots \bullet \text{---} \text{---} \text{---} \text{---} \dots = N g^2 T \frac{d-1}{d} p^i \int_{\mathbf{k}} \frac{1}{\mathbf{k}^4} \quad (\text{D.10})$$

$$\text{Diagram: } \dots \bullet \text{---} \text{---} \text{---} \text{---} \dots + \text{Diagram: } \dots \bullet \text{---} \text{---} \text{---} \text{---} \dots = -N g^2 T (d-1) p^i \int_{\mathbf{k}} \frac{1}{\mathbf{k}^4} \left( c_1 G_t(0, \mathbf{k}) - \frac{1}{d} \right) \quad (\text{D.11})$$

$$\text{Diagram: } \dots \bullet \text{---} \text{---} \text{---} \text{---} \dots = -N g^2 T c_1 (d-1) p^i \int_{\mathbf{k}} \frac{1}{\mathbf{k}^4} G_t(0, \mathbf{k}) \quad (\text{D.12})$$

the sum of which gives

$$-\Pi_{\lambda A^0}^i = \dots \text{---} \text{---} \text{---} \text{---} \dots = 2 N g^2 T (d-1) p^i \int_{\mathbf{k}} \frac{1}{\mathbf{k}^4} \left( \frac{1}{d} - c_1 G_t(0, \mathbf{k}) \right). \quad (\text{D.13})$$

## References

- [1] A. D. Linde, Phys. Lett. **B96** (1980) 289; D. J. Gross, R. D. Pisarski, L. G. Yaffe, Rev. Mod. Phys. **53** (1981) 43.
- [2] E. Braaten and A. Nieto, “Free Energy of QCD at High Temperature,” Phys. Rev. D **53** (1996) 3421 [arXiv:hep-ph/9510408].
- [3] For a recent review of leptogenesis, see W. Buchmüller, “Recent progress in leptogenesis,” arXiv:hep-ph/0107153.
- [4] For a review of electroweak baryon number violation and baryogenesis see, e.g., V.A. Rubakov, M.E. Shaposhnikov, Usp. Fis. Nauk **166** (1996) 493 [arXiv:hep-ph/9603208].
- [5] L. D. McLerran, E. Mottola and M. E. Shaposhnikov, “SPHALERONS AND AXION DYNAMICS IN HIGH TEMPERATURE QCD,” Phys. Rev. D **43** (1991) 2027.

- [6] G. D. Moore, “Electroweak bubble wall friction: Analytic results,” *JHEP* **0003** (2000) 006 [arXiv:hep-ph/0001274].
- [7] G.D. Moore, “Sphaleron rate in the symmetric electroweak phase,” *Phys. Rev. D* **62**, 085011 (2000)[arXiv:hep-ph/0001216].
- [8] Y. Nakahara, M. Asakawa and T. Hatsuda, “Hadronic spectral functions in lattice QCD,” *Phys. Rev. D* **60** (1999) 091503 [arXiv:hep-lat/9905034]; F. Karsch, E. Laermann, P. Petreczky, S. Stickan and I. Wetzorke, “A lattice calculation of thermal dilepton rates,” *Phys. Lett. B* **530** (2002) 147 [arXiv:hep-lat/0110208].
- [9] E. Braaten and R. Pisarski, *Nucl. Phys. B* **337** (1990) 569; *Phys. Rev. D* **45** (1992) 1827; J. Frenkel and J.C. Taylor, *Nucl. Phys. B* **334** (1990) 199; J.C. Taylor and S.M.H. Wong, *Nucl. Phys. B* **346** (1990) 115; J. P. Blaizot, E. Iancu, “Soft collective excitations in hot gauge theories,” *Nucl. Phys. B* **417**, 608 (1994) hep-ph/9306294; V.P. Nair, “Hard thermal loops, gauged WZNW action and the energy of hot *Phys. Rev. D* **48**, 3432 (1993) hep-ph/9307326.
- [10] D. Y. Grigoriev and V. A. Rubakov, “Soliton Pair Creation At Finite Temperatures. Numerical Study In (1+1)-Dimensions,” *Nucl. Phys. B* **299** (1988) 67; J. Ambjørn, M. L. Laursen and M. E. Shaposhnikov, “Baryon Asymmetry Generation In The Electroweak Theory: A Lattice Study,” *Nucl. Phys. B* **316** (1989) 483.
- [11] G. D. Moore, C. r. Hu and B. Müller, “Chern-Simons number diffusion with hard thermal loops,” *Phys. Rev. D* **58** (1998) 045001 [arXiv:hep-ph/9710436].
- [12] G. D. Moore and K. Rummukainen, “Classical sphaleron rate on fine lattices,” *Phys. Rev. D* **61** (2000) 105008 [arXiv:hep-ph/9906259].
- [13] D. Bödeker, G. D. Moore and K. Rummukainen, “Chern-Simons number diffusion and hard thermal loops on the lattice,” *Phys. Rev. D* **61** (2000) 056003 [arXiv:hep-ph/9907545].
- [14] D. Bödeker, L. D. McLerran and A. Smilga, “Really computing nonperturbative real time correlation functions,” *Phys. Rev. D* **52** (1995) 4675 [arXiv:hep-th/9504123].

- [15] D. Bödeker, “A local Langevin equation for slow long-distance modes of hot non-Abelian gauge fields,” *Phys. Lett. B* **516**, 175 (2001) [arXiv:hep-ph/0012304].
- [16] D. Bödeker, “On the effective dynamics of soft non-abelian gauge fields at finite temperature,” *Phys. Lett. B* **426**, 351 (1998) [arXiv:hep-ph/9801430].
- [17] G. D. Moore, “The sphaleron rate: Boedeker’s leading log,” *Nucl. Phys. B* **568**, 367 (2000) [arXiv:hep-ph/9810313].
- [18] D. Bödeker, “Diagrammatic approach to soft non-Abelian dynamics at high temperature,” *Nucl. Phys. B* **566** (2000) 402 [arXiv:hep-ph/9903478].
- [19] J. P. Blaizot and E. Iancu, “Ultrasoft amplitudes in hot QCD,” *Nucl. Phys. B* **570** (2000) 326 [arXiv:hep-ph/9906485].
- [20] P. Arnold, “An effective theory for  $\omega \ll k \ll gT$  color dynamics in hot non-Abelian plasmas,” *Phys. Rev. D* **62** (2000) 036003 [arXiv:hep-ph/9912307].
- [21] P. Arnold and L. G. Yaffe, “Non-perturbative dynamics of hot non-Abelian gauge fields: Beyond leading log approximation,” *Phys. Rev. D* **62** (2000) 125013 [arXiv:hep-ph/9912305]; “High temperature color conductivity at next-to-leading log order,” *Phys. Rev. D* **62** (2000) 125014 [arXiv:hep-ph/9912306].
- [22] For a review, see e.g. J. Zinn-Justin, “Quantum Field Theory And Critical Phenomena,” *Oxford, UK: Clarendon (1989) 914 p. (International series of monographs on physics, 77)*.
- [23] J. Zinn-Justin and D. Zwanziger, *Nucl. Phys. B* **295** (1988) 297.
- [24] D. Bödeker, “From hard thermal loops to Langevin dynamics,” *Nucl. Phys. B* **559** (1999) 502 [arXiv:hep-ph/9905239].
- [25] See e.g. P. H. Damgaard and H. Hüffel, “Stochastic Quantization,” *Phys. Rept.* **152**, 227 (1987).